Design and Stabilization of a One Legged Hopping Robot

B.Tech. Project

of

Pratik Chaudhari

Roll No : 06D01015

under the guidance of

Prof. Hemendra Arya
Department of Aerospace Engineering, IIT Bombay.

and

Prof. Bhartendu Seth
Department of Mechanical Engineering, IIT Bombay.

Indian Institute of Technology Bombay
December 13, 2009

Contents

Abstract

Single-legged locomotion gait is a hopping motion consisting of alternate flight and stance phases. In such a hopping robot, if the energy lost in friction and impacts is compensated, then along with control of robot attitude we can have stable hopping motion.

An offset-mass hopping robot is a novel idea in the realm of single-legged robots. These robots have an inherent tendency to leap forward due to the offset mass which eases the requirement of effort from the actuators. A reaction wheel is necessary to ensure that we can have a stable gait for different horizontal velocities and initial conditions. This project aims to build a prototype of a SLOM one legged hopper and its reaction wheel mechanism to demonstrate a stable 2D hopping gait.

The structure of this report is as follows,

- Chapter 1 introduces the one legged hopper problem along with a discussion of previous work in this area. It focusses on the different energy pumping mechanisms and balancing techniques used.
- Chapter 2 details previous work done at IIT Bombay on the SLOM hopper and motivates the problem statement for the current project through this discussion.
- Chapter 3 talks about two different mechanical designs for the SLOM hopper. A qualitative analysis of both the designs is provided along with pointers for the choice of mechanisms of the final design from among them.
- We look at three major aspects of hopper design in Chapter 4. It provides an analysis of the 2 mass problem, frequency modes and reaction wheel stabilization to ultimately choose the design values for the masses and the motors.
- A brief introduction of the embedded platform on the hopper is provided in Chaper 5. It provides results of the testing of a Kalman filter for the IMU using actual sensors. We also look at velocity control of a motor with quadrature encoders at the end.

Keywords:
SLOM, offset-mass, energy-pumping, hopping robot, height control, reaction wheel, attitude control, Kalman filter, inertial measurement unit

List of Figures

Chapter 1

Introduction

The motivation for research in legged robotics has been to understand human motion and legged motion in general. There are various applications that spring to mind when one thinks of the uses of legged robots viz. travelling on difficult terrain, search and rescue operations in event of fires and landslides, space exploration etc. At the same time it fulfils the science fiction dream of having a running and jumping robotic pet! Some of the major challenges in development of legged robots are, [1]

1. Stronger energy pumping mechanisms are needed to compensate the energy loss after impact with the ground. Heavier the robot, more energy is lost every impact which results in larger and even heavier actuators to compensate it.

2. Dynamics of legged robots is significantly more complex than wheeled ones. Control strategies employed for different actions like hopping and running are much different from each other.

3. Energy efficiency is a major concern due to multiplying effect of any extra weight added to the robot.

1.1 Previous approaches

Marc Raibert pioneered the field of legged robotics [2, 3]. He developed three pneumatically actuated one legged robots to demonstrate 3D hopping. There have been a variety of approaches towards building better actuators and stabilization strategies. We shall look at them briefly in the following sections. Sayyad, Seth and Seshu review the development of one legged robots in detail in this review paper [1].

1.1.1 Energy pumping

Pneumatic actuators as energy pumping mechanism were seen in Raibert's *Monopod* [4] and Zeglin's *Uniroo* [5]. It was observed that electro-mechanical actuators were much more efficient than pneumatic or hydraulic actuators. Papantoniou used a cable transmission system to actuate the leg and body linkage using a spring traction mechanism [6]. There was a series of hoppers named ARL Monopods developed by Buehler [7, 8] that utilized a ball-screw

mechanism to store energy in a leg spring. ARL Monopods also demonstrated a stable running gait and significantly better energy characteristics. Zeglin built a planar bow-legged hopper wherein a flexible bow shaped leg was compressed and positioned using servomotors [9]. This was a completely self-sufficient and light robot with onboard batteries. Almost all approaches after this have used springs to store energy and provide impact forces for liftoff; only major differences being whether they used springs in a telescopic leg or as a part of the joints in an articulate leg.

1.1.2 Stability

Different designs of hoppers can be divided into actively balanced robots and passively balanced robots.

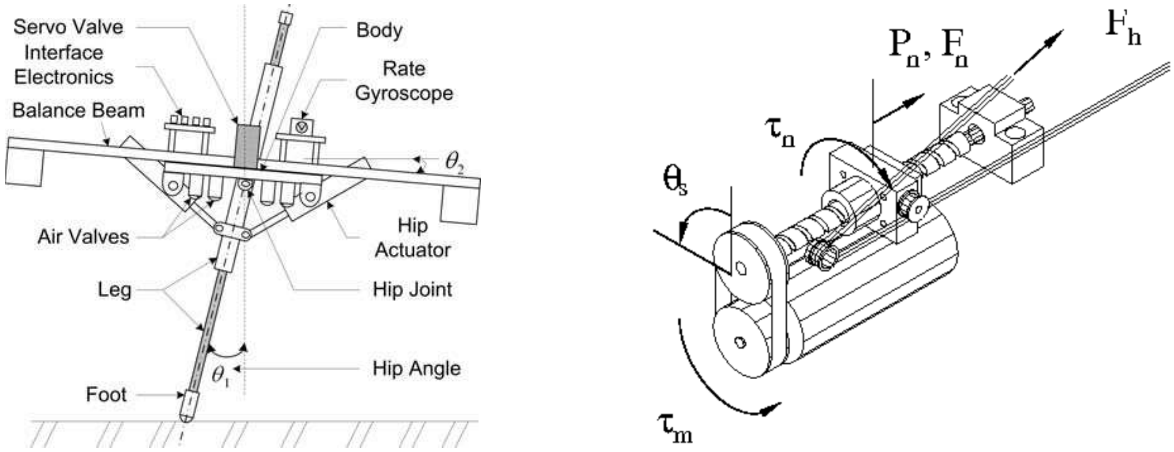

(a) Raibert 2-D Hopper [1]

(b) ARL Monopod I [7]

Figure 1.1: Actively stabilized hoppers

Actively Balanced Robots

Raibert used a hydraulically actuated hip on top of an articulate leg mechanism for balancing the hopper. The hip actuator used in the two-dimensional hopper shown in Fig. 1.1a was pneumatically controlled by varying the pressure gauged by pressure sensors on the actuators. The hip can also be moved by means of a winch type actuator as shown in Fig. 1.1b.

Passive Balancing Robots

Swinging the leg for active balancing requires energy and people started looking for ways to achieve passive stabilization of hopper attitude. This kind of stabilization might not provide a complete solution to the problem of stability but certainly reduces the power consumption of the robot. After studying ARL Monopod I, Beuhler incorporated a compliant spring in series with the hip actuator cables as shown in Fig. 1.2a. Swinging of the leg could be achieved using the hip-leg spring compliance. Thus a passively stable running gait was possible for certain initial conditions [10, 8].

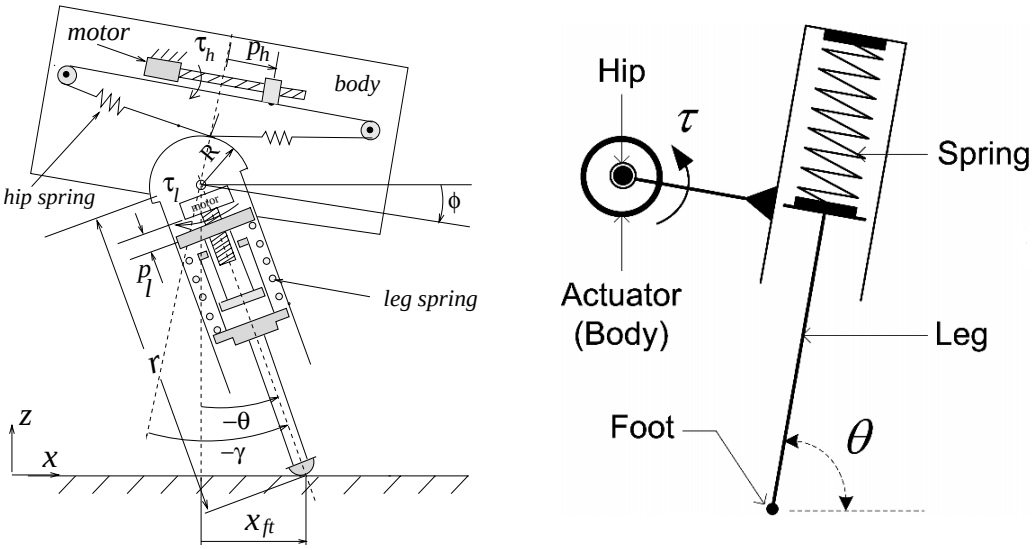

(a) ARL Monopod II [8] (b) SLOM hopper [11]

Figure 1.2: Passively dynamically stable hoppers

Most of the hoppers reviewed in [1] have their C.G. along the line of action of the impact and spring forces. This provides a stable system for single place hopping and is referred to as *Springy Leg Inverted Pendulum* (SLIP). It is noted that SLIP does not account for the pitch stabilization problem which is of practical concern.

As shown in Fig. 1.2b, Shanmuganathan et. al. considered asymmetric configurations in which the CG location was offset from the geometric center. This is referred to as a *Springy-Legged Offset-Mass* (SLOM) hopper [12]. The robot postures at various phases during a hopping cycle are depicted in Fig. 4.6. The impulsive torque acting during the stance gives a pitch up velocity in the flight phase. This compensates the net pitch down during the stance phase due to the horizontal velocity. Sayyad and Seth have analyzed this configuration using a 3D Poincaré map to obtain a periodic motion stabilized by observer based state feedback strategy [11]. Fig. 1.3 shows a miniature 5 cmm tall SLOM hopper developed by Wei et. al. [13]

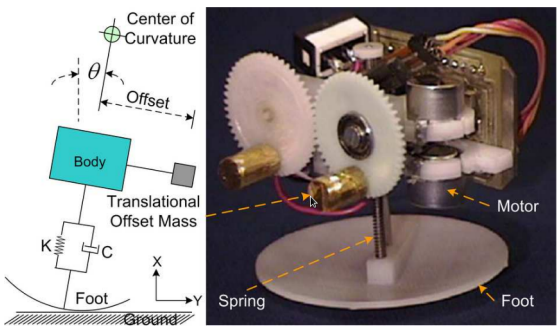

Figure 1.3: 5 cm tall hopper by Wei et. al. [13]

Chapter 2

Problem Statement

This chapter discusses previous work on the one legged hopper at IIT Bombay and formulates the exact problem statement and the scope for this project.

2.1 Previous work

2.1.1 1-D Hopper

Vitthal Londhe [14] developed a 1D hopper and demonstrated in place hopping capabilities. The design was aimed at minimizing the energy losses and making the robot easy to assemble and disassemble.

Fig. 2.1, shows the major parts of this hopper viz. a winding motor with the energy pumping mechanism and a telescopic leg with a ratchet and paul constraint. The hopper is also confined to a fixed vertical axis. The leg is connected to a compression spring. A motor is used to compress this spring.

The constraint mechanism consists of a bell crank attached to the paul so that when the leg impacts upon the ground, the paul comes free of the ratchet teeth and the spring is free to compress further. This is the first use of impact forces for releasing the energy pumping mechanism in a one legged hopper. Thus the motor does not need to do work against the spring force to hold the leg in the compressed position. The latch mechanism mechanically latches the leg in place and unlatches it only when the leg touches the ground.

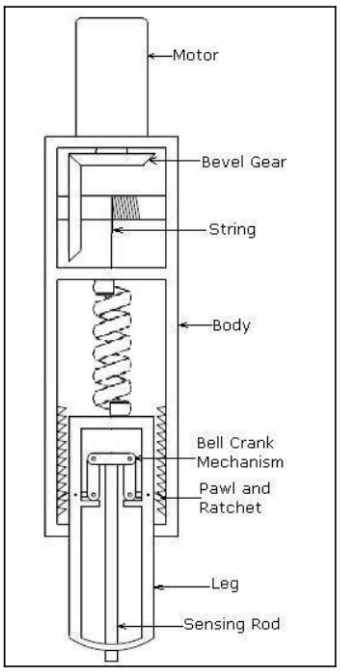

Figure 2.1: Vertical Hopper [14]

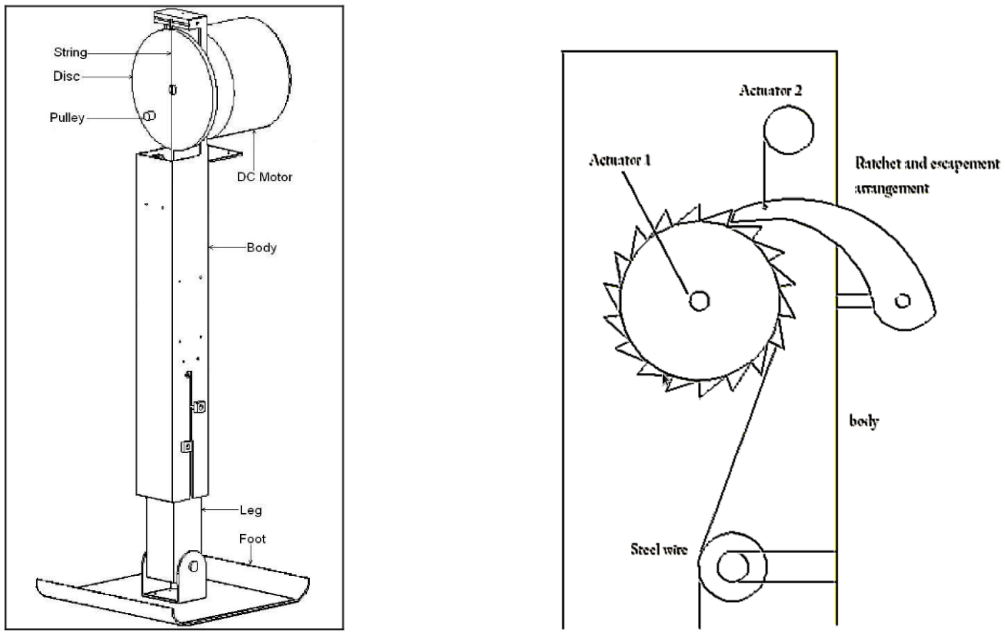

(a) SLOM hopper : sketch

(b) Paul and ratchet

Figure 2.2: 2D SLOM hopper [15]

2.1.2 SLOM Hopper

Fig. 2.2a shows the prototype developed by Sharma and Gebretsadik [14] for which Vipul Saboo [15] designed and fabricated the EPM for it. He could also demonstrate hopping of the robot without active balancing.

The robot consists of a body and a telescopic leg of rectangular cross-section attached to the body by a spring. The leg also has a freely rotating ankle with a foot attached to it. The ankle ensures that the foot always falls flat on the ground irrespective of the orientation of the robot while touchdown.

To reduce the friction between the telescopic leg and the body, teflon bearings are used in sets of two on each of the four sides of the leg. The construction of the robot makes it very difficult to assemble and disassemble it. Also, the mass of the leg is almost $2/3^{rd}$ of the mass of the body which results in huge energy loss of the system during impacts. The EPM consists of a ratchet and a pawl with a voice-coil which activates the pawl. The voice-coil is electrically actuated by a mechanical limit switch attached on the foot of the robot. There is also a latch-type EPM where the motor can be switched off after the spring is compressed.

Simit [16] developed a treadmill and constraining mechanism (TCM) for the SLOM hopper. He also demonstrated an embedded system for hopping height control using a feed-forward and PID controller. A ground station for gathering telemetry data from the TCM interface.

2.1.3 Reaction wheel

Siraj [17] modeled attitude control of the hopper as a position control problem for the reaction wheel pendulum. He demonstrated PID and LQR control strategies for the reaction wheel pen-

dulum. Optimal control strategies have to be looked into because as observed by Beuhler [10, 8], almost 50% of the total energy is utilized in swinging the leg mass i.e. in attitude reorientation. A inertial measurement unit (IMU) using a complementary filter was also developed.

2.2 Problem formulation

The SLOM hopper was used as a test bed for devising hopping strategies by Saboo [15], Simit [16] and Siraj [17]. However, it was an over-designed system with large energy losses due to impacts and friction. It was necessary to remove these flaws in the robot before further work could be done on it. Hence, it was decided to go ahead with a completely new mechanical design for the hopper keeping the following things in mind about the previous design.

1. SLOM concept is quite novel and the new design will be based on it.
2. Compression spring need an enclosure outside them to keep them in place when in compression. This results in frictional losses in every cycle of energy pumping. Tension springs on the other hand do not have such frictional losses associated with them. It was thus decided to use tension springs for the new design.
3. The SLOM hopper could not hop above a height of 10 cm. The energy pumping mechanism (EPM) was the limiting factor. For achieving heights larger than this, we need to significantly reduce the leg mass and have a more energy efficient EPM.
4. A reaction wheel should be present on the hopper and this will be used to reorient the robot to demonstrate both in-place hopping and running capabilities.
5. An embedded system along with on-board power supply shall be used to control the actuation, sensors and execute the control law.

Chapter 3

Mechanical Design

As pointed out in the previous chapter, the major task of this project was to devise an efficient mechanical design. Two different designs both based on extension springs were looked into. This chapter describes them and the motivation behind choosing the final design to be fabricated.

3.1 Design 1

Energy pumping

Fig. 3.1 shows the pulley mechanism for storing energy in the large central spring. The winding motor is placed upon the platform which can be called as the larger mass M of the two mass system. A winch connects the motor to the same platform passing over the pulley on the lower leg. Thus, as the motor rotates, it pulls the platform (and itself) downwards while extending the spring above it.

Constraint

Fig. 3.1 also shows the constraint mechanism for the pulley. It consists of a hatch connected to the lower leg with a torsional spring. The toothed part of the pulley is free to move in the clockwise direction (thus compressing the torsional spring every time). The lower part of the leg is cylindrical with a top flange which matches the top face of the cylindrical bushing shown inside the main leg. Thus the lower leg can move only up. The protruding portion of the main leg prevents the hatch from moving in the clockwise direction, thus constraining the pulley from rolling back in the anti-clockwise direction.

Using the impact for energy release

This design is unique because it utilizes the impact force ($m\ v_{touch-down}$) to release the stored energy in the main spring. Visualize the lower leg impacting on the ground. This results in the hatch (which is holding the pulley from moving back) impacting against the protrusion of the main leg. Since the impact force is easily larger than the torsional spring force, the hatch closes and the lower leg goes inside the main leg thus enabling free rotation of the pulley. There is a compression spring inside the main leg connected to the lower leg which gets compressed while this happens. It is responsible for pushing the lower leg back outside after $t_{liftoff}$.

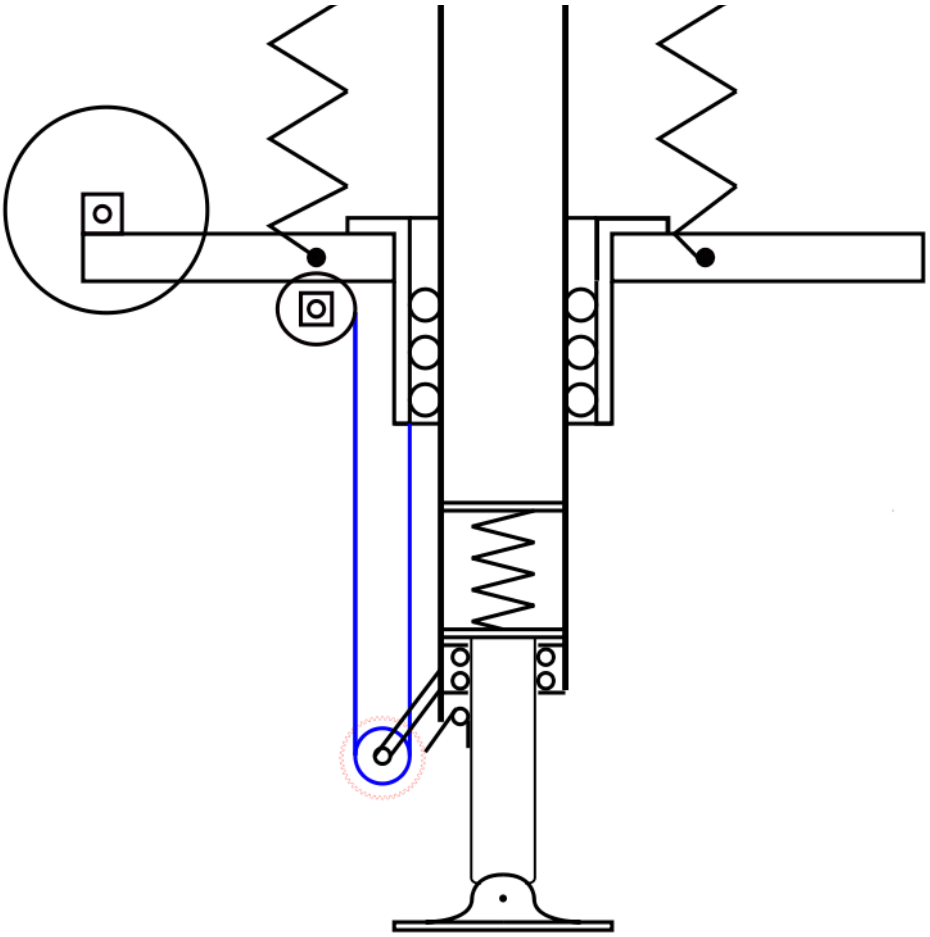

Figure 3.1: Winding motor with pulley on the leg

3.1.1 Evaluation

- The motor has to move a distance twice that of the extension of the spring. This is especially important when we look at the timescales over which we have to extend the spring, these are around 200-300 msecs. A larger distance in smaller time results in a large ω for the motor which translates to a smaller available torque. This necessitates a larger motor that can provide this torque.

- The large mass of the platform (M) is helping in the extension of the spring and hence the torque required for the winding motor reduces.

- It has to be ensured that the winding winch does not slip over the pulley when the platform is suddenly released from the constraint. At the same time, the winch must be free enough so as not to hinder the movement of the platform after the release.

- The platform moves over the leg with the help of a circular bushing. There is another bushing for the lower leg to move into the upper leg. These circular bushings are light and durable.

3.2 Design 2

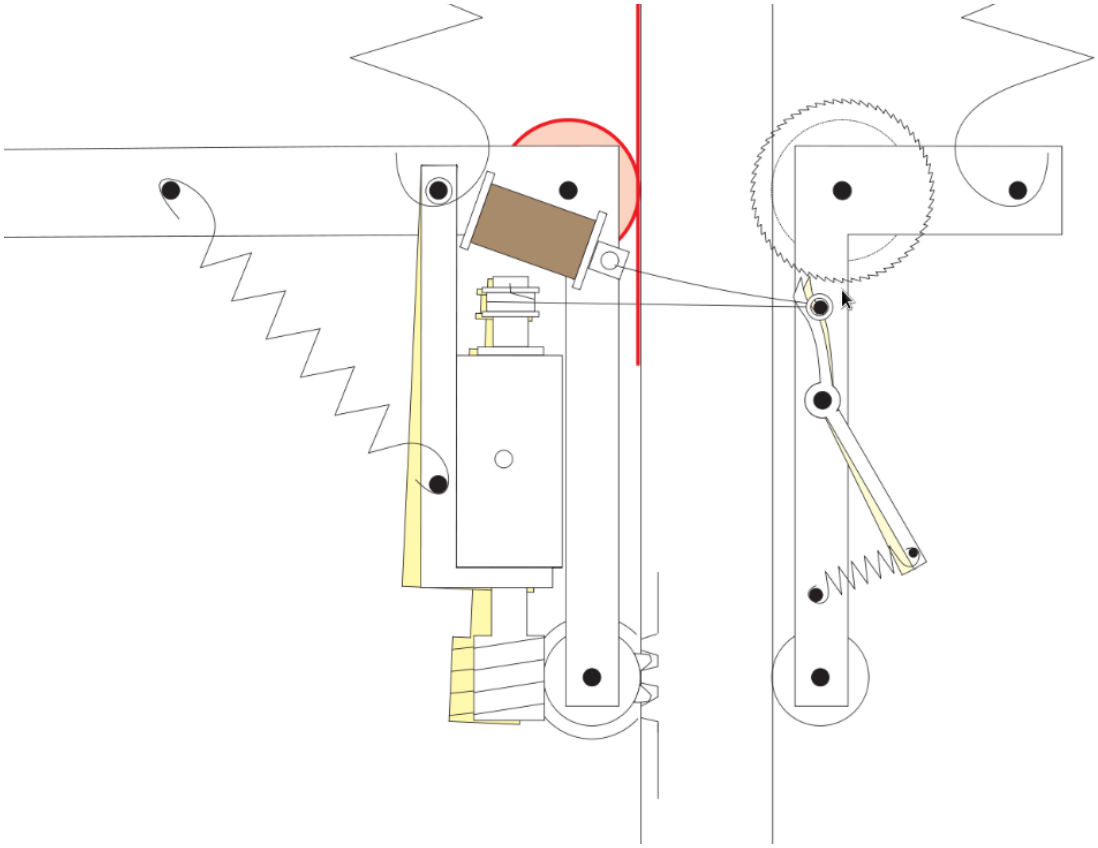

Figure 3.2: Rack and pinion on the leg with the drive motor

Energy pumping

Fig. 3.2 shows another design that was considered. The leg consists of a rack on one of its sides. A single dual shaft motor in a sleeve is used to drive the pinion on this rack as well as pull the paul to free the ratchet. This motor consists of a string attached to a friction pulley on the shaft. A friction pulley is a device whose coupling is dependent upon the speed of the relative motion between the two surfaces. Thus, the motor can pull the paul only beyond a certain ω. Below this speed, the paul spring is strong enough to engage it with the ratchet. After the paul engages, the string becomes slack again.

Constraint

The platform and the ratchet are rigidly connected to a band drive which rolls along the length of the leg. This ensures that contact of the roller inside the band drive and the leg is maintained at all times. Since the ratchet is rigidly connected to the platform, both can only move together i.e. only when the paul is pulled by the drive motor.

Energy release

This design uses an electromechanical system to release energy. After sensing the impact through a touch switch located below the leg, we can use a voice coil actuator to pull the string which in turn moves the paul. This brings in the pull back spring attached to the sleeve into the picture and it promptly pulls the sleeve away from the rack. Note that the string attached to the drive motor pulley is slack at this point.

3.2.1 Evaluation

- The sleeve of the motor is kept on the same side as that of the reaction wheel and helps to provide an offset mass for the SLOM effect. The body mass also helps to obtain an offset C.G.; thus the distance of the reaction wheel from the axis need not as be as large as calculated in Section 4.3.
- The worm-worm wheel on the rack mechanism provides a huge mechanical advantage and thus reduces the maximum torque required from the motor. This scales down the mechanical system as well as the electronic system requirements.
- All the force of the extension springs is coming as an axial load on the shaft of the motor. We thus need to choose a gearbox that can handle these axial loads.
- The friction pulley has to work against the pual spring, sleeve spring and the horizontal component of the rack force ($k\,x\,tan\,\theta$) to keep the string in tension. This is compounded by the fact that the there is a maximum ω the motor can accelerate to in the energy storing phase. It is much better if this ω is dictated by the torque requirements which are as critical rather than this mechanism.
- Less resolution on the desirable extension of springs because we are operating on a rack. This can however be easily taken care of in the pitch control law.
- The constraint mechanism for Design 2 is not reliable enough and should be improved upon. The major problem is to provide an opposing force to the horizontal component of the rack–worm-wheel force ($k\,x\,tan\,\theta$). This force has to be present when the motor is extending the springs and should be removed before we release the ratchet so that the platform along with the motor-sleeve is free to move up. To disengage the motor from the rack, the spring shown in the left part of Fig. 3.2 will have to be there as well.

Chapter 4

Sizing of Hardware

We looked at two designs in Chapter 3. This chapter describes some simulations done for the sizing of various components. The major parts of this process are,

1. Masses of the platform and the leg
2. Dimensions of the reaction wheel based on the above masses
3. Choice of winding and reaction wheel motors

4.1 2 mass problem

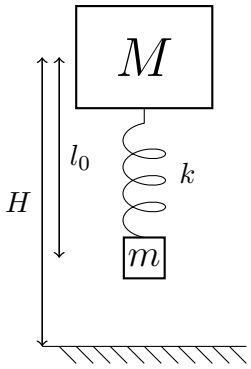

Figure 4.1: 2 mass problem [16]

The basic idea behind a hopper is like that of the 2 masses connected by a spring problem. If the system shown in Fig. 4.1 is allowed to fall from a height, the heavier mass pulls the smaller mass with it back into the air after impact. Every cycle is accompanied by a loss in energy due to the inelastic impact of the smaller mass with the ground. If we pump this energy back into the system using an external agent in every cycle, we can ensure sustained hopping at the chosen height. The 2 mass problem can thus be taken as a basis to compute the range of values of masses for acceptable performance. The following assumptions have been used in the simulation that follows,

1. Dropping height (H) : 0.6 m

2. Spring constant (k) : 300 N/m

3. Spring relaxed length (l_0) : 0.3 m

4. Trapezoidal profile for ω of the winding motor (constant α at the start and end)

5. Design 1 was used as the base for this simulation. It is expected that the total torque requirements will reduce due to the mechanical advantage provided by the rack and pinion design as shown in Fig. 3.2.

6. Neglect energy loss due to friction

It is seen from Fig. 4.1 that if h_i are progressive heights, we have the relation,

$$h_n = \frac{Mh_{n-1} + ml_0}{M + m} \tag{4.1}$$

$$E_{loss} = \frac{Mg\,(H - l_0)}{1 + M/m} \tag{4.2}$$

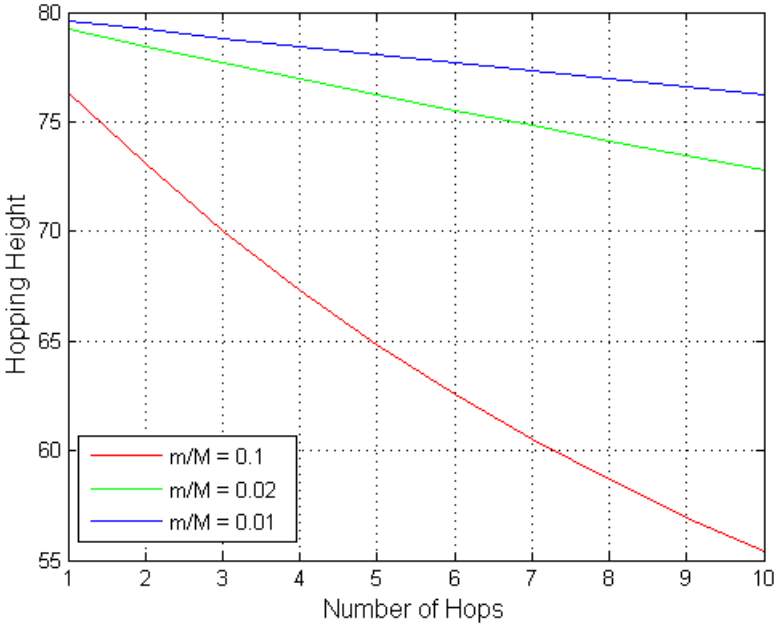

Figure 4.2: Hopping height for different M/m

From Fig. 4.2, it is seen that larger the ratio M/m, i.e. smaller the leg mass, less is the loss in energy resulting in more number of hops. This is also seen for a increasing M. We would however, like the M to be within limit too as we will also need to pump in extra energy into the system if the desired hopping height is more than the starting height.

Fig. 4.3 shows the required torque for extending springs to compensate the energy lost during impact fully within 0.2 sec. This simulation has been plotted for Design 1 from Chapter 3 with a pulley radius of 2 cms. It is observed that m is the single most important parameter in hopper design. The required torque is a very strong function of the leg mass. As this mass increases, we

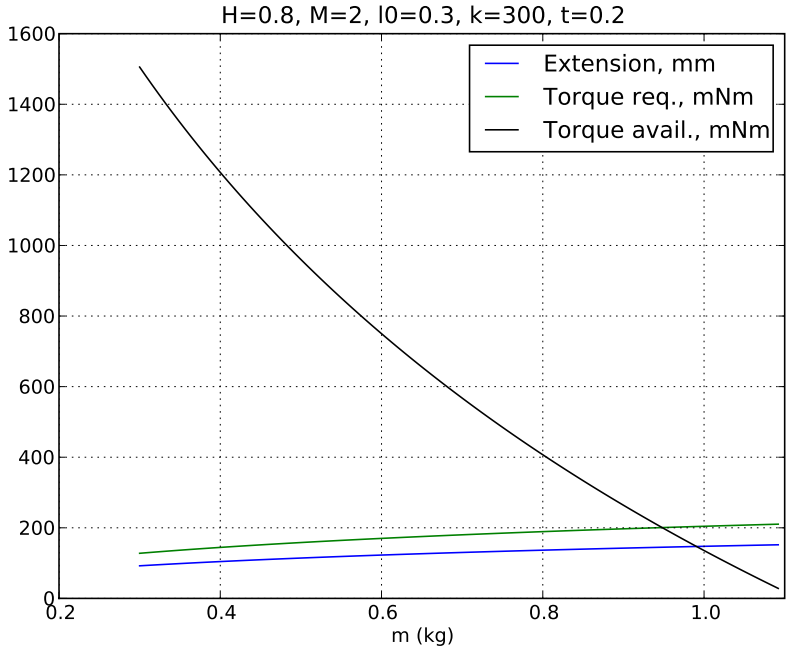

Figure 4.3: Torque variation with m

need a larger motor to satisfy torque requirements. It is noted that a value of about 0.4–0.6 kg can be called a reasonable estimate for the leg mass as we can easily choose a motor delivering the required torque for these values.

It is also seen that an extension of about 11 cms with a single spring of k = 300 Nm is needed to compensate the energy loss for hopping heights of 80 cms. So we should ensure that we can provide a maximum extension around 15 cms.

4.2 Impact analysis

The desired hopping height dictates a hopping frequency. Intuitively, smaller hopping height results in large number of impacts per time and consequently in larger energy loss per unit time. This is seen from Fig. 4.4 because the hopping frequency is closer to the natural frequency for small hopping heights. However, beyond this consideration, since the hopper is a spring mass system, it possesses a natural frequency of its own. If the hopping frequency is near to this natural frequency, a large amount of energy is taken away by impact forces in every cycle. We intend to arrive at a range of values for the masses to ensure a large difference between the hopping frequency (ω_{hop}) and the natural frequency (ω_{nat}). The details of this analysis are as follows,

- Conserve energy at H and the moment of maximum extension of the spring after $t_{touchdown}$ to get the minimum height of the fully extended platform above the leg. This comes out to be 8 cms for m = 0.4 kg. This value also reduces with increasing m. I assumed no pre-extension of the spring while calculating this. The final value will be less then 8 cms

if we take it into account. Thus we say that the leg should protrude about 12 cms beyond the maximum extension of the platform which is obtained from Fig. 4.2.

- If x_2 is the height of C.G. just before touchdown, we can calculate the time taken for it to fall from a height H to x_2 as t_1.
- M undergoes simple harmonic motion from time t_1 till liftoff, and this time of motion is t_2
- M transfers its momentum at $t_1 + t_2$ to m resulting in a velocity v_{cg,t_2} for the C.G. To ensure that M has largest velocity while transferring momentum to m, we need to put a mechanical stopper at the natural length of the spring.
- The resultant velocity is just enough for the C.G. to reach a height H in time t_3.
- Total hopping time T $= t_1 + t_2 + t_3$, with $\omega_{hop} = \frac{2\pi}{T}$.
- $\omega_{nat} = \sqrt{\frac{k\,(1+m/M)}{m}}$

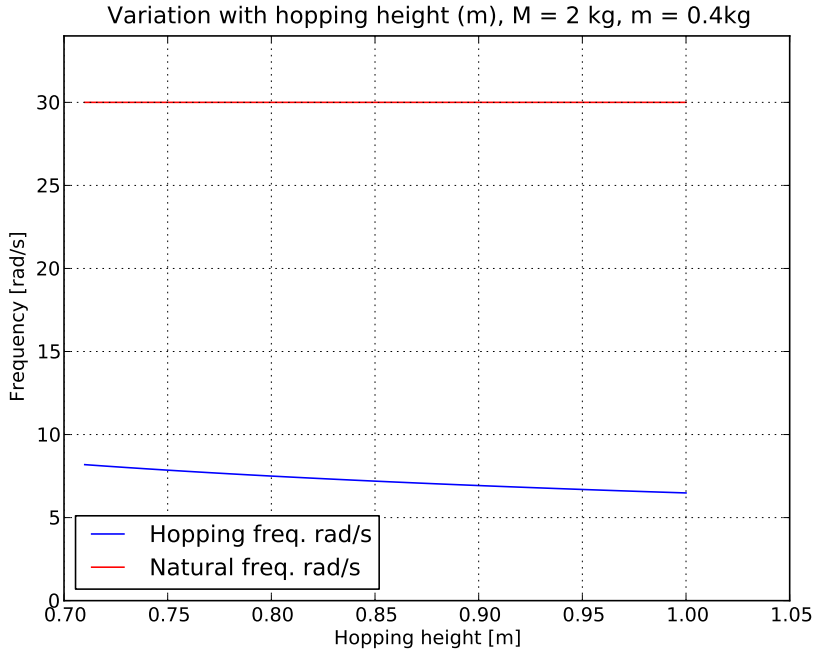

Figure 4.4: Frequency variation with hopping height for M/m = 5

Fig. 4.4 shows that ω_{hop} and ω_{nat} are separated by large gap for the usable range of values of hopping height. A similar analysis for variation of M also reveals that the two frequencies are separated by a large gap for all usual values. Fig. 4.5 succinctly depicts all the above analysis. As the leg mass increases, the hopping frequency goes closer to the natural frequency i.e. more impact per unit time. To compound matters, more and more energy is lost per impact as per Eqn. 4.2. So the conclusion from impact analysis is that the leg mass should be as low as possible. It is also seen from Fig. 4.5 that m = 0.4 – 0.6 kg is a good solution as well as an achievable one.

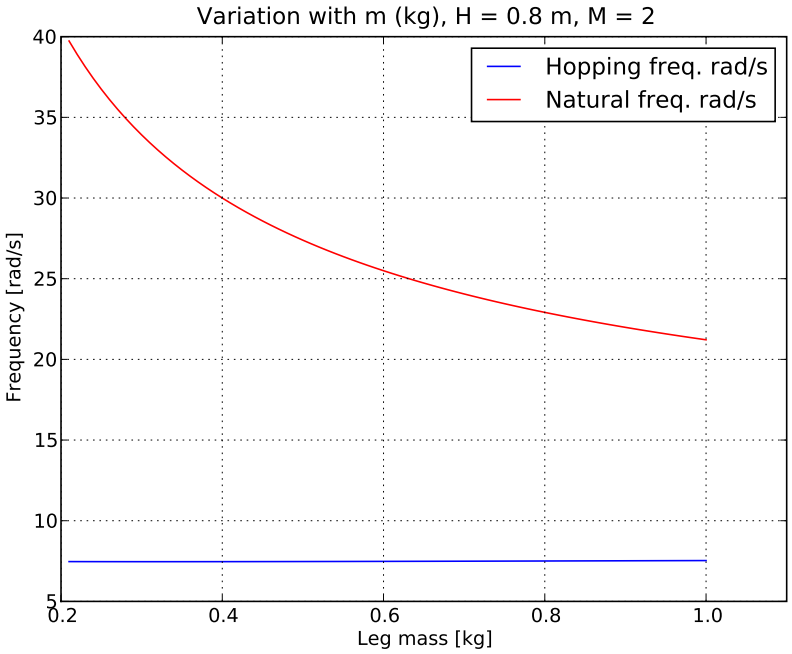

Figure 4.5: Frequency variation with m

4.3 Reaction wheel

For achieving a running gait with the hopper, it has to be started with the exact initial pitch and horizontal velocity. For any other initial condition, the hopper is pitch unstable and will not be able to continue the running gait. As mentioned in [12], an offset mass acts as a passive stabilization to the pitch attitude of the hopper. To get rid of this need for exact initial condition which is quite impractical, we design a reaction wheel on the hopper. This will result in torque coupling on the pitch axis and thus provide an active control over the pitch of the robot. The coupling equation can be written as,

$$J_{wheel}\ \omega_{wheel} = -(J_{wheel} + J_{body})\ \omega_{body} \tag{4.3}$$

Let us look at the various stages of reaction wheel stabilization,

- Let θ_{impact} be the impact pitch attitude and $\theta_{liftoff}$ be the lift-off attitude. Pitch is measured with respect to the vertical direction. An upright hopper means a pitch of zero.
- From Fig. 4.6, the stabilizing impact torque is given by $\tau = m\ v_{impact}\ (h_{cg} sin\ \theta + d_{cg} cos\ \theta)$. This is a positive torque and generates a pitch up. Also, $\omega_{liftoff} = \tau_{impact}\ / J_{body}$
- The angle rotated due to horizontal velocity in the stance phase is $\Delta\ \theta = -v_h\ / h_{cg}\ \Delta\ t$ where v_h is the horizontal velocity. This means $\theta_{liftoff} = \theta_{impact} + \Delta\ \theta$.
- The lift-off pitch needs to be corrected to θ_{impact} while the hopper is in the air. $\omega_{liftoff}$ might not be enough to correct this pitch and so we need an additional reaction wheel.

The following assumptions were made during the analysis for the reaction wheel,

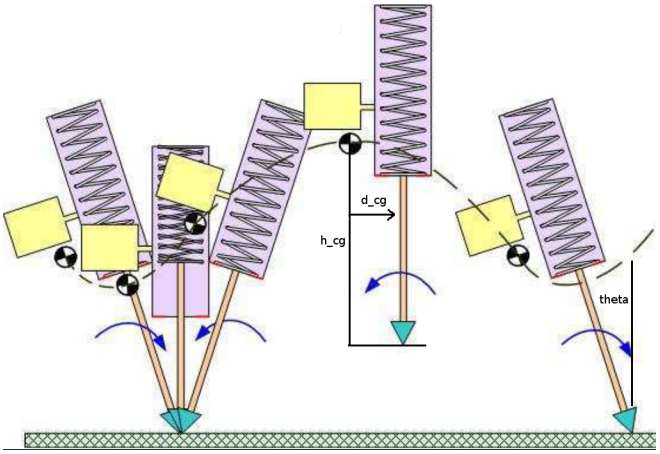

Figure 4.6: Stabilizing impact torque due to SLOM

- The reaction wheel is taken as a ring with mass of 1.5 kg concentrated at the rim.
- It is easy to see that for any given horizontal velocity, there exists a particular impact pitch which results in stable gait without a reaction wheel. Our objective is thus to go to this impact pitch angle from any given initial condition such as a zero pitch angle.
- We consider the case where the pitch is such that we have no horizontal velocity and no stabilization impulse from the ground. This pitch is reoriented to 30 degrees within one hop which corresponds to a huge horizontal velocity of 13.5 m/s. The stable pitch will be less than this for lower velocities. In actual operation there will be large reaction wheel torques only while converting the initial condition into a stable running gait. After that there will only be small control torques about the stable pitch angle.
- We assume a trapezoidal profile for ω_{wheel} with length of the plateau taken as $T_{air}/2$. The acceleration phase is $T_{air}/5$ on either side. This means that we finish the reorientation task within 9/10 ths of the time that the hopper remains in the air in the first hop ($T_{air} = t_1 + t_3$ from Section 4.2).

Results

Figs. 4.7 and 4.8 have been plotted for distance of C.G. = 6 cms and radius of the reaction wheel taken as 6 cm (mass = 1.5 kg). We can see that the required torque for reorientation as mentioned in above is around 500 mNm with output power being around 1.5 W.

4.4 Choosing Components

Reaction wheel motor

Figs. 4.8 and 4.7, were plotted for a 2342CR024 motor. We bump up the gear ratio to achieve a higher available torque as compared to the necessary torque. There is a trade off here because we also want a particular value of ω for reorientation. We thus choose to suffer on the amount of

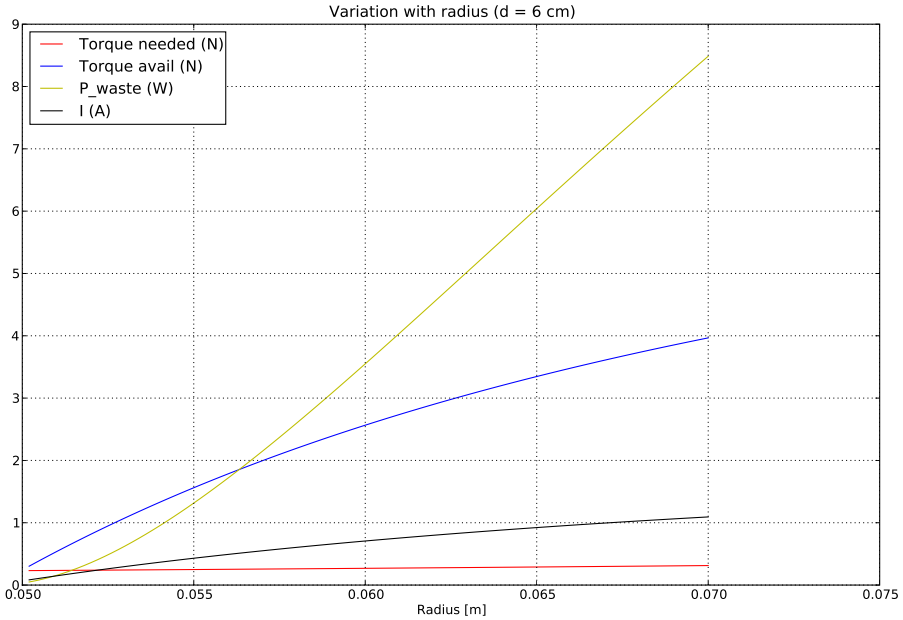

Figure 4.7: Torque requirements vs wheel radius

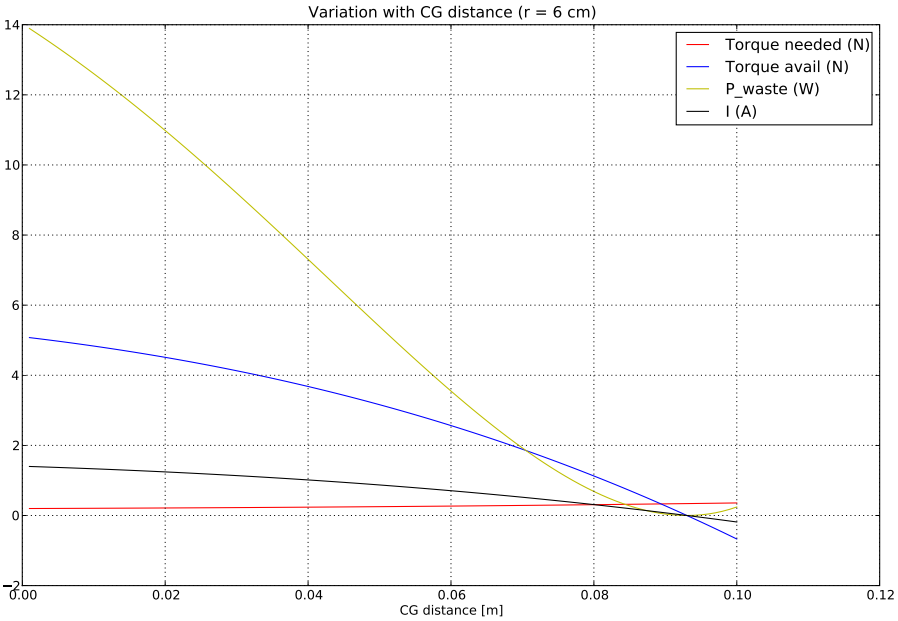

Figure 4.8: Torque requirements vs C.G. offset

wasted power to achieve these dual objectives. The gear-box thus chosen is one with a standard $139:1$ ratio. The motor was chosen by looking at the currents required for different motors. The current required for this motor is around 1.2 A.

Drive motor

We look at Fig. 4.3 to choose the drive motor. For the purposes of design, we take common values of worm-worm wheel diamter ratio (0.5), pressure angle (20 deg), helix angle for worm (25 deg) and co-efficient of friction $\mu = 0.3$. The torque required from the motor is not more than 200 mNm. The total power required for this task is about 4.5 W. We choose the same 2342CR024 motor for this task. The gear box is taken as a $43:1$ standard one to ensure that we are operating at the rated motor speed. This results in less energy wastage. There need not be any optical encoders for this motor as we will be measuring the velocity of the extension using encoders at the band drive. The currents for this operation are always below 1.5 A. Hence we can use a relatively small motor driver like Texas Instruments DRV 8801 to drive this motor.

Chapter 5

Embedded System

This chapter details the development of the embedded system necessary for controlling and actuating the hopper. It consists of two major parts,

1. Micro-controller and RF interface
2. Inertial Measurement Unit (IMU)

5.1 Micro-controller

The micro-controller chosen for this system is a Microchip dsPIC33F64MC804. It can run at 40 MIPS with an onboard flash memory of 64 KB along with a 16 KB SRAM. There are a host of integrated peripherals like Serial Peripheral Interface (SPI), UART, Analog to Digital converter (ADC), Quadrature Encoder (QEI) and timers to generate Pulse Width Modulation (PWM) that can be used for motor control. Other major features provided with it are the Direct Memory Access controller (DMA) which can transfer memory from one peripheral to other without CPU intervention and the high multiplexing of its IO pins. The latter enables almost all IO pins to be assigned to any of the above mentioned peripherals (except analog pins) and greatly simplifies design. Pickit 2 is a programmer cum debugger that had been ordered for programming the micro-controller.

XBee modules using the Zigbee protocol are used to form a wireless link with the embedded system on the hopper. The range of these devices is quite sufficient for indoor uses (about 100 m). The interface on the micro-controller side is through UART and a custom made FT232 module will be used to interface it with the base station to gather telemetry. A python module to grab and plot this telemetry from the virtual serial port of FT232 is in development.

The current development board contains one motor driver and its adjoining encoder port. The final module will contain two motor drivers and encoder arrangements for the pinion and the reaction wheel motors.

5.2 Inertial Measurement Unit (IMU)

5.2.1 Hardware

We need to read the current pitch of the hopper for proper reorientation before every hop. This is done with the help of an IMU. It consists of a two-axis accelerometer (ADIS 16201) and a single axis gyroscope (ADIS 16255). Both provide 14-bit signed readings via the SPI interface with internal temperature bias compensation for the gyroscope. Using a digital sensor has benefits over an analog output sensor because the ADC of the micro-controller can give a maximum resolution of only 12 bits as compared to the 14-bit reading given by these sensors.

The sensitivity of the gyroscope is 0.07326 ^{o}/s/LSB for the whole range of $\pm$ 320 ^{o}/s with a noise of 0.48 ^{o}/s. The accelerometer has a sensitivity of 2.162 LSB/mg with a noise of 22 LSB. The accelerometer also consists of an inclinometer to measure the angle with respect to the ground. However, it provides a sensitivity of only 10 LSB/deg. This necessitates the need of onboard inverse tangent tables to get the pitch angle from accelerometer readings. The bandwidth of the gyroscope is 50 Hz as compared to 2.25 kHz of the accelerometer. This severely limits the update rate of the filter and hence we need a better gyroscope.

5.2.2 Kalman Filter

As shown in Fig. 5.1, the readings of the gyroscope and the accelerometer are highly noisy and erratic even in the situation of smooth movements of the IMU. This shows, that depending upon either of the two sensors is not good for pitch estimation. Gyroscopes are high frequency sensors and accurately estimate the rate. However, they also show pronounced variation of readings with time (gyro bias) and temperature (compensated to an extent). Accelerometers are good at low frequency measurements. These do not suffer from a growing bias like the gyroscopes and can be used to correct the readings estimated on the basis of gyroscope rate from time to time. We look at Kalman filter as a way to fuse these two sensors.

Various alternatives for filtering schemes exist and complementary filters are very widely used for fusing accelerometers and gyroscopes on IMUs. I decided to use a Kalman filter because the micro-controller can easily handle the computations at usable update rates of about 20-50 Hz. This is one of the major reasons cited in literature for the use of complementary filters over Kalman filters [18]. It is also noted that for linear systems, there is little difference in the equations of the two filters.

The equations for Kalman filter with a state vector $\boldsymbol{x} = [x_1 \;\; x_2]^T = [\theta \;\; \dot{\theta}]^T$ are give below [19].

State equation :

$$\boldsymbol{x}_{k+1} = \boldsymbol{A}\,\boldsymbol{x}_k + \boldsymbol{B}\,\boldsymbol{u}_k + \boldsymbol{w}_k \tag{5.1}$$

Output equation :

$$y_{k+1} = \boldsymbol{C}\,\boldsymbol{x}_{k+1} + z_{k+1} \tag{5.2}$$

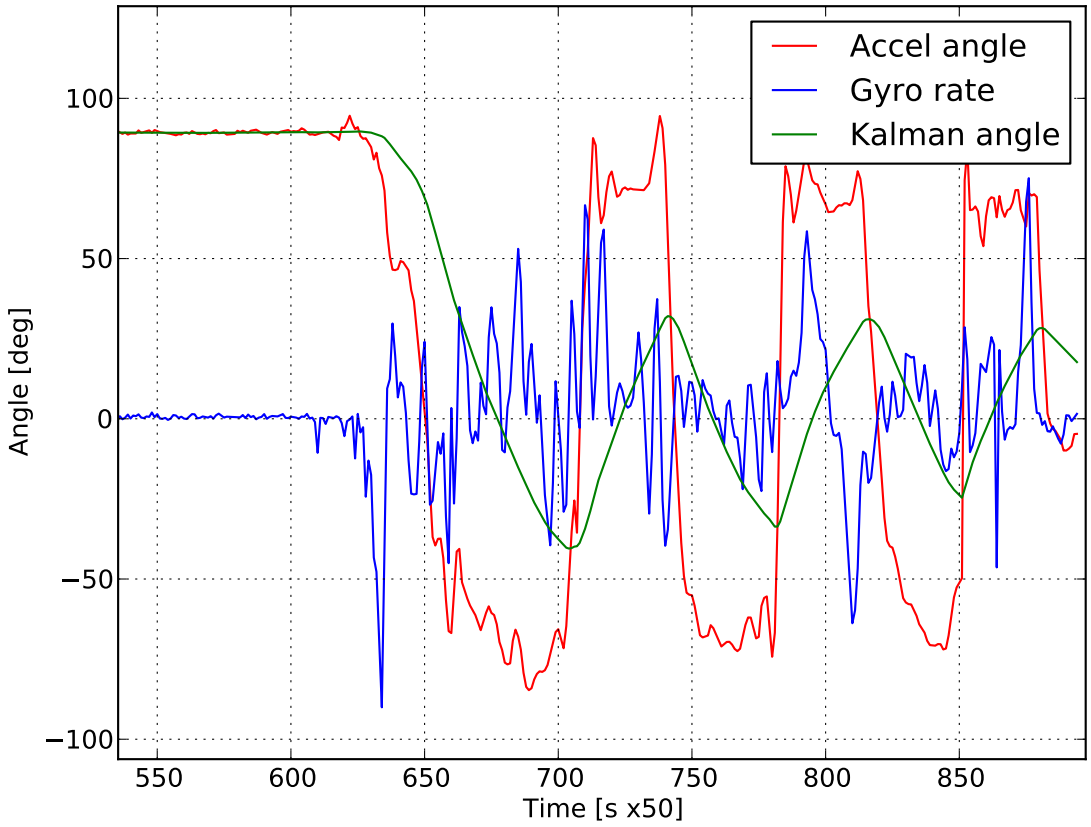

Figure 5.1: Kalman filter : Low frequency input

Update equations :

$$\boldsymbol{K}_k = \boldsymbol{A}\,\boldsymbol{P}_k\,\boldsymbol{C}^T\,\left(\boldsymbol{C}\,\boldsymbol{P}_k\,\boldsymbol{C}^T + S_z\right)^{-1} \tag{5.3}$$

$$\hat{\boldsymbol{x}}_{k+1} = (\boldsymbol{A}\,\hat{\boldsymbol{x}}_k + \boldsymbol{B}\,\boldsymbol{u}_k) + \boldsymbol{K}_k\,(y_{k+1} - \boldsymbol{C}\,\hat{\boldsymbol{x}}_k) \tag{5.4}$$

$$\boldsymbol{P}_{k+1} = \boldsymbol{A}\,\boldsymbol{P}_k\,\boldsymbol{A}^T + \boldsymbol{S}_w - \boldsymbol{A}\,\boldsymbol{P}_k\,\boldsymbol{C}^T\,S_z^{-1}\,\boldsymbol{C}\,\boldsymbol{P}_k\,\boldsymbol{A}^T \tag{5.5}$$

For our state vector, the equations consist of,

$$\boldsymbol{A} = \begin{bmatrix} 1 & dt \\ 0 & 1 \end{bmatrix} \quad \boldsymbol{B} = \begin{bmatrix} dt \\ 0 \end{bmatrix} \quad \boldsymbol{u} = \begin{bmatrix} \dot{\theta}_{gyro} \\ 0 \end{bmatrix} \quad y = \theta_{accel} \quad \boldsymbol{C} = \begin{bmatrix} 1 \\ 0 \end{bmatrix} \tag{5.6}$$

$\boldsymbol{P}$ is called the estimation error co-variance and can be initialized to some value, a small value implies that we expect the error co-variance to be small too. We assume that the estimation errors are completely dependent upon one another and hence initialize the matrix as identity. S_z is the accelerometer variance obtained from the datasheet. $\boldsymbol{S}_w$ is the gyroscope covariance matrix. Let $\nu_{angle} = dt\,\sigma_{rate}$ and $\nu_{rate} = 0$. These values are thus obtained from the datasheet

for a particular filter update rate.

$$\boldsymbol{P} = \begin{bmatrix} 1 & 0 \\ 0 & 1 \end{bmatrix} \quad \boldsymbol{S}_w = \begin{bmatrix} \nu_{angle}^2 & \nu_{angle}\,\nu_{rate} \\ \nu_{angle}\,\nu_{rate} & \nu_{rate}^2 \end{bmatrix} = \begin{bmatrix} 92 \times 10^{-6} & 0 \\ 0 & 0 \end{bmatrix} \tag{5.7}$$

Eqns. 5.1 – 5.4 were converted to their algebraic form instead of the matrix operations for better calculation speed. Fig. 5.1 shows the performance of this filter with calculations being done on the computer. Fixed-point arithmetic has been implemented on the micro-controller and will be used for the onboard Kalman filter.

Results

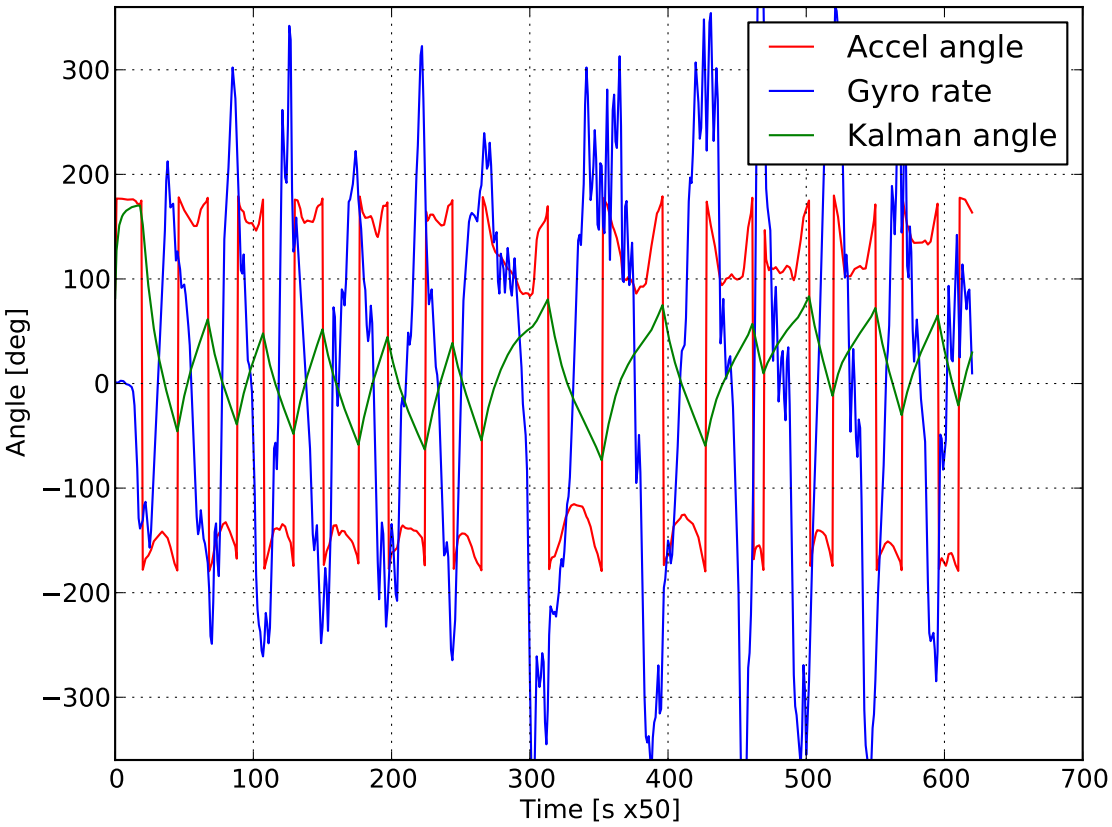

Figure 5.2: Kalman filter : High frequency input

Fig. 5.2 has been plotted for a very high frequency movement of the IMU. As shown, the rates exceed $\pm 320^o/s$ which is the maximum rate detected by the gyro. The final output of the kalman filter does match the hand movement of about 90 degrees. However, at about the 300^{th} update, it completely misses a very fast 360 deg. rotation of the IMU. This is reasonable because even the accelerometer and gyroscope do not seem to significantly register this movement.

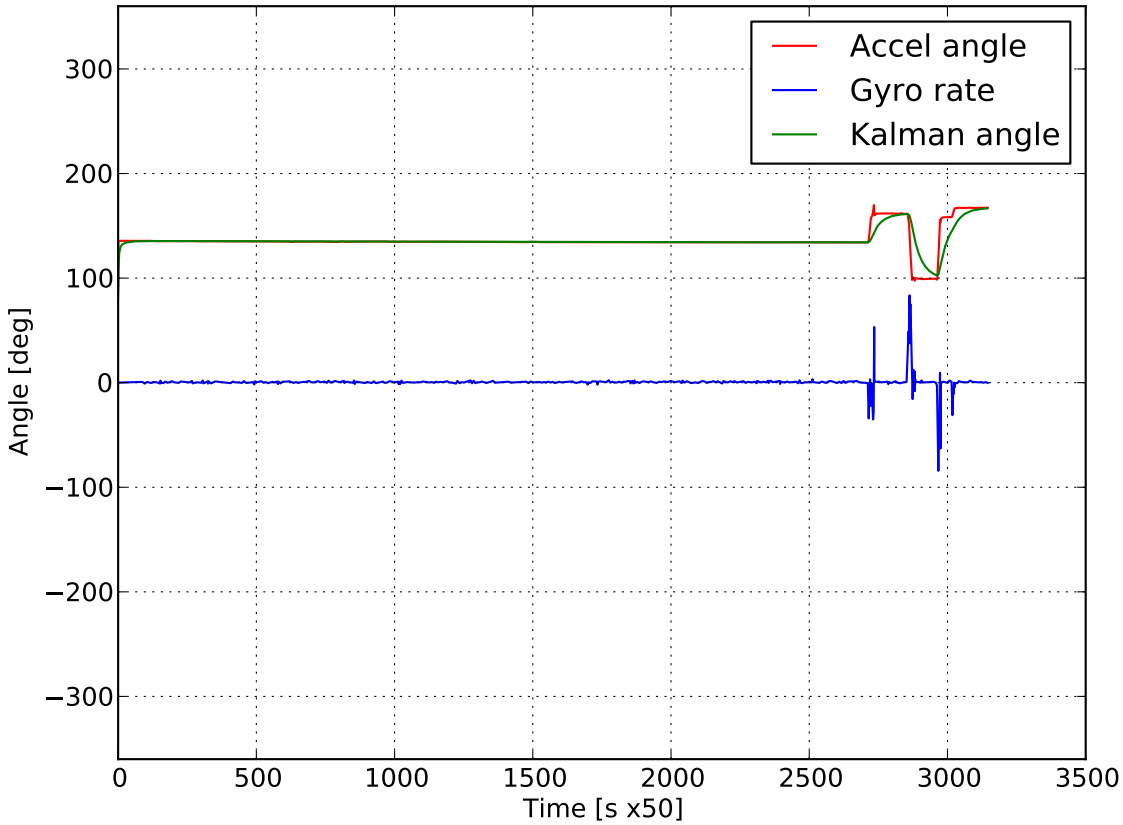

Figure 5.3: Kalman filter : Gyro drift

Fig. 5.3 shows readings plotted for 5 minutes at a 10 Hz update rate for the filter. It is seen that the gyro rate has some noise. However, integrating this noise does not show a large error in the angle moved by the sensor. The integral of the gyro rate is zero for all the time. The drift mentioned for gyroscopes is not to be seen even for periods as large as 12 minutes.

Chapter 6

Future Work

Mechanical design

This report discussed two mechanical designs that we formulated to try to obtain an efficient energy pumping mechanism for the one legged hopper robot. Both the designs have their share of flaws and it is not possible to go ahead with the fabrication without further analysis on any one of them. A few lessons from this effort and the sizing analysis for the hopper have become pretty clear such as the need of a rack and pinion mechanism, effects of a large leg mass on the hopping dynamics and general torque considerations for the whole hopper.

The reaction wheel stabilization part can be designed almost independently from the rest of the mechanism. The selection of the reaction wheel dimensions and its motor is thus finished. Future changes in the hopping design will only marginally change these numbers.

Thus future work involves demonstrating running and in-place hopping capabilities using the TCM and treadmill designed by Simit [16].

Embedded system

The IMU is almost complete and we just need to ask a few questions whether just pitch attitude is sufficient for us. The above mentioned constraint (TCM) should ensure that we do not need to add sensors to determine roll and yaw angles. A final hopper board will have to be designed having two motor drivers for the EPM and reaction wheel motors. This will also contain the IMU and the wireless XBee interface on it.

Control strategy

We need to formulate a control law for hopping height control. The pitch orientation control law can be developed on the same lines of Siraj [17] which has already been implemented by him earlier. Integrating these two control laws to demonstrate a running gait will result in a hopping robot which can be used as a platform for further work in control dynamics of hoppers, path following [9] and uneven terrain.

References

[1] A. Sayyad, B. Seth, and P. Seshu, "Single-legged hopping robotics research — A review," *Robotica*, vol. 25, no. 5, pp. 587–613, 2007.

[2] . http://www.ai.mit.edu/projects/leglab, Last checked on November 4, "MIT Leg Lab."

[3] M. H. Raibert, "Legged robots," *Communications of ACM*, vol. 29, no. 6, pp. 499–514, 1986.

[4] W. Lee and M. Raibert, "Control of hoof rolling in an articulated leg," *Robotics and Automation, 1991. Proceedings., 1991 IEEE International Conference on*, pp. 1386–1391, 1991.

[5] G. Zeglin, "Uniroo: A One-Legged Dynamic Hopping Robot," tech. rep., Massachusetts Institute of Technology, 1991.

[6] K. Papantoniou, "Electromechanical design for an electrically powered, actively balanced one leg planar robot," *Intelligent Robots and Systems '91. 'Intelligence for Mechanical Systems, Proceedings IROS '91. IEEE/RSJ International Workshop on*, pp. 1553–1560 vol.3, Nov 1991.

[7] P. Gregorio, "Design, Control and Energy Minimization Strategies for the ARL Monopod," Master's thesis, McGill University, 1994.

[8] M. Ahmadi and M. Buehler, "Preliminary Experiments with an Actively Tuned Passive Dynamic Running Robot," *Experimental Robotics V*, 1997.

[9] J.-C. Zufferey, "First Jumps of the 3D Bow Leg Hopper," tech. rep., The Robotics Institute, Carnegie Mellon University, 2001.

[10] M. Ahmadi and M. Buehler, "A control strategy for stable passive running," *Proc. IEEE/RSJ Conf. on Intelligent Robots and Systems*, vol. 3, pp. 152–157, 1995.

[11] A. Sayyad, *Dynamics and Control of a Single Legged Offset Mass Hopping System.* PhD thesis, Indian Institude of Technology Bombay, Dept. of Mechanical Engineering, 2007.

[12] P. Shanmuganathan, *Dynamics and Stabilization of Under-Actuated Monopedal Hopping.* PhD thesis, Indian Institude of Technology Bombay, Dept. of Mechanical Engineering, July 2002.

[13] T. Wei, G. Nelson, R. Quinn, H. Verma, and S. Garverick, "Design of a 5-cm monopod hopping robot," *Robotics and Automation, 2000. Proceedings. ICRA'00. IEEE International Conference on*, vol. 3, 2000.

[14] V. N. Londhe, "Energy Pumping Mechanism for Hopping Robot," tech. rep., Indian Institute of Technology, Bombay, 2007.

[15] V. Saboo, "Development of a Hopping Robot," tech. rep., Indian Institute of Technology, Bombay, 2008.

[16] S. Pradhan, "Prototype Development for Hopping Height Control of a One-Legged Hopping Robot," tech. rep., Indian Institute of Technology, Bombay, 2009.

[17] S. Issani, "Design and Implementation of Reaction Wheel Mechanism to Control a One-legged Hoppng Robot," tech. rep., Indian Institute of Technology, Bombay, 2009.

[18] W. Higgins(Jr.), "A Comparison of Complementary and Kalman Filtering," *Aerospace and Electronic systems, IEEE Transactions on*, vol. 11, no. 3, 1975.

[19] G. M. and A. A., *Kalman Filtering : Theory and Practice.* John Wiley and Sons Inc., 2001.